Globular Dendrimers Involving a C_{60} Core and a Tetraphenyl Porphyrin Function

Xavier Camps,[a] Elke Dietel,[a] Andreas Hirsch,*[a] Soomi Pyo,[b] Luis Echegoyen,*[b] Steffen Hackbarth,[c] and Beate Röder*[c]

Abstract: A series of highly compact globular dendrimers, **5**, **21**, and **22**, involving a C_{60} core with a T_h symmetrical addition pattern was synthesized by way of the fivefold cyclopropanation of the fullerene–porphyrin dyad **2** with dendritic malonates in the remaining octahedral positions. Whereas **5** contains classical Fréchet benzyl-ether-based systems, a new type of dendra containing a flexible spacer between the branching units was developed for the synthesis of **21** and **22**. The spectroscopic, electrochemical, and photophysical properties of the tetraphenylporphyrin–zinc (Zn-TPP) chromophore within the functional dendrimers depend not only on the presence but also on the generation number of the surrounding dendra and therefore on the nanoenvironment provided by the neighboring addends. This is reflected, for example, in the bathochromic shifts of the Soret and Q-bands of the porphyrin moiety and in the shift of the first reduction potentials to more negative values for both the fullerene and porphyrin moieties with increasing generation number. Whereas in the dyad **2** a photoinduced electron transfer from the porphyrin to the fullerene can occur, dendrimers **21** and **22** show fluorescence properties and singlet oxygen formation properties ($\Phi_\Delta = 0.66-0.67$) reminiscent to those of the parent Zn-TPP.

Keywords: dendrimers · electrochemistry · fullerenes · porphyrins · singlet oxygen

Introduction

The development of functional dendrimers is a new and promising concept in supramolecular science.[1] The very first examples of applications using carefully designed dendritic systems range from macromolecular recognition, catalysis ('dendrizymes'), light harvesting, energy transduction to new mesogenic behavior.[1] As a result, it was suggested that dendritic porphyrins could act as model systems for natural electron transfer heme proteins like cytochrome c or hemoglobin.[2, 3] Using suitable branches, it should be possible to modulate the electrochemical redox activity of the inner electrophore. This modulation is attributed to strong nanoenvironmental effects and differences in solvation imposed on the electroactive core by the densely packed dendritic surroundings. A few systems where porphyrins were used as cores for dendrimers have been reported.[2–5] For example, Inoue and co-workers describe an interesting molecule, where eight fourth-generation dendritic branches are connected to a porphyrin core.[2] Diederich and co-workers have reported a water-soluble second-generation dendritic Fe^{III} porphyrin, which has a redox potential for the biologically relevant Fe^{III}/Fe^{II} couple in water that is shifted by 420 mV. The shift results from the nature of the dendritic wedges.[3]

High-valent metalloporphyrins have also been employed as catalysts for the oxidation of organic substrates.[6] Introduction of bulky dendritic polymers at the peripheral positions of a metal porphyrin results in steric protection of the metal center, which could lead to regio- and shape-selective catalytic behavior.[5] Although such dendrimer–porphyrins showed significantly greater regioselectivity than the corresponding unhindered parent metalloporphyrin, the selectivity so far has not been as high as those achieved with other crowded bis-pocket porphyrins like 5,10,15,20-tetrakis(2′,4′,6′-triphenylphenyl)porphyrin.[6]

Recently, we showed that C_{60} can be used as a versatile building block for the facile construction of globular dendrimers, for example **1**,[8] containing benzyl ether-based dendra introduced by Fréchet et al.[9] In order to investigate charge transfer processes between these two electrophores,

[a] Prof. Dr. A. Hirsch, Dr. X. Camps, Dipl.-Chem. E. Dietel
Institut für Organische Chemie
Henkestrasse 42, D-91054 Erlangen (Germany)
Fax: (+49) 9131-85-26864
E-mail: hirsch@organik.uni-erlangen.de

[b] Prof. Dr. L. Echegoyen, S. Pyo
Department of Chemistry, University of Miami
Coral Gables, FL 33124 (USA)
Fax: (+1) 305-284-4571
E-Mail: echegoyen@miami.edu

[c] Prof. Dr. B. Röder, Dipl.-Phys. S. Hackbarth
Institut für Physik, Humboldt-Universität Berlin
Invalidenstrasse 110, D-10115 Berlin (Germany)

0947-6539/99/0508-2362 $ 17.50+.50/0

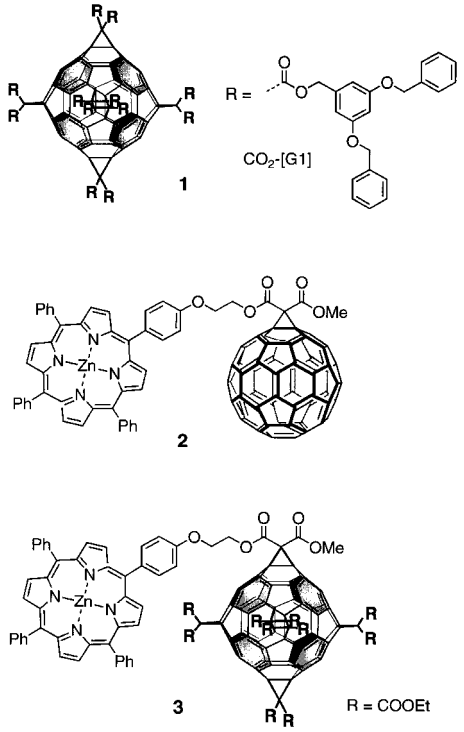

we and others are involved in the synthesis of fullerene–porphyrin dyads like **2**.[10] In our approach, a variety of mono- and bifunctional tetraphenylporphyrin precursors were covalently linked to C_{60} by means of nucleophilic cyclopropanation.[10n, r] We now propose a new concept of functional dendrimers (Figure 1), which is based on our experience with

Abstract in German: *Wir berichten über eine Serie von hochkompakten, globulären Dendrimeren **5**, **21** und **22**, die einen C_{60}-Kern mit einem T_h-symmetrischen Additionsmuster enthalten. Ihre Synthese erfolgte durch fünffache Cyclopropanierung oktahedraler Positionen der Fulleren-Porphyrin–Diade **2** mit dendritischen Malonaten. Verbindung **5** enthält Fréchets klassische Benzylether-Dendronen. Für die Synthese von **21** und **22** wurde ein neuer Typ von Dendronen entwickelt bei denen flexible Spacereinheiten zwischen den Verzweigungen eingefügt sind. Die spektroskopischen, elektrochemischen und photophysikalischen Eigenschaften des Zink-Tetraphenylporphyrin (ZnTPP)-Chromophors innerhalb dieser funktionalen Dendrimere werden von der Anwesenheit der Dendronen und auch von deren Größe beeinflußt. Dieser Einfluß der Nanoumgebung auf den Metallmakrocyclus macht sich zum Beispiel in der bathochromen Verschiebung der Soret- und Q-Banden des Porphyrins und in der Verschiebung der ersten Reduktionspotentiale sowohl des Porphyrin- als auch des Fullerenteils zu negativeren Werten mit steigender Generationszahl bemerkbar. Während für **2** ein photoinduzierter Elektronentransfer vom Porphyrin zum Fulleren gefunden wird, zeigen die funktionalen Dendrimere **21** und **22** Fluoreszenz- und Singulettsauerstoffgenerierungseigenschaften ($\Phi_\Delta = 0.66–0.67$), die mit dem von ZnTPP vergleichbar sind.*

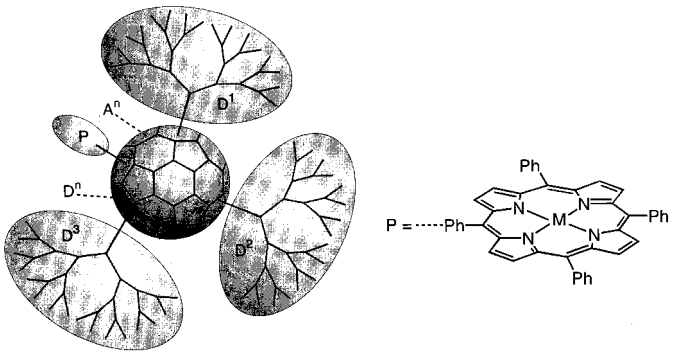

Figure 1. Schematic representation of functional dendrimers involving the C_{60} core as a structure determining building block and a tetraphenyl porphyrin as a functional unit. D^1, D^2, D^3, … D^n denote identical or dissimilar dendra. The A moieties are additional addends which may also be attached to the core. They may have another function or they may be just positional blockers, which enable the easy construction of a given addition pattern within the fullerene core.

fullerene dendrimers, fullerene–porphyrin dyads, and the regioselective formation of mixed hexakisadducts like **3**.

Starting from a dyad such as **2**, a highly compact globular dendrimer with a T_h-symmetrical addition pattern of the fullerene core should be easily accessible by fivefold cyclopropanation of the remaining octahedral positions. The cyclopropanation is carried out using dendritic malonates and our template-mediation method.[11] In this prototype of a functional dendrimer, the fullerene core would act just as a structure-determining building block, since it is to be expected that in the remaining π-conjugated skeleton the characteristic electrophoric properties of C_{60}[12] are lost. The dendra provide a specific and widely adjustable microenvironment around the porphyrin, thus modulating its electrochemical and coordination properties. The porphyrin–fullerene distance can be fine-tuned by choosing the proper linkage to go between them. Since other addition patterns are also easily accessible, different types and numbers of dendritic branches can be introduced in the neighborhood of the metal site. With the right combination of building blocks, the porphyrin can be surrounded by dendra but can still be available for reactions like coordination of axial ligands to the metal center. This accessibility might be very useful when designing catalysts or mimicking hemoproteins like cytochrome 450, which regulate oxygen activation and insertion into organic substrates.

In spite of its success, our synthetic strategy for the construction of fullerene dendrimers has some limitations. Although the synthesis of highly compact hexakisadducts containing up to ten and twelve[8] first-generation benzyl ether-type dendra has been accomplished, these compounds were obtained only in low yields as a consequence of the steric hindrance involved in their formation processes. In order to build up globular fullerene-based architectures mimicking the size and shape of natural macromolecules, it is crucial to develop alternative methodologies for the synthesis of C_{60} hexakisadducts containing higher generation dendritic branches. We present for the first time the synthesis, characterization, and the electrochemical and photophysical properties of a series of functional dendrimers (Figure 1). In order to circumvent the problem of steric hindrance during

the convergent binding of classical Fréchet type dendra, we developed a new type of more flexible dendra by applying the concept of hyperbranched cores (*hypercores*).[13–17]

Results and Discussion

The syntheses of the fullerene–porphyrin dendrimers were carried out by fivefold cyclopropanations of the monoadduct **2** at the octahedral sites. These regioselective reactions can be promoted by using the template-activation method that we developed previously.[11] For this purpose, the auxiliary addend 9,10-dimethylanthracene (DMA) undergoes reversible [4+2] cycloadditions causing an activation of free [6,6] double bonds in octahedral sites accessible for irreversible attacks of malonates. It was expected that the yields of such convergent syntheses would strongly depend on the bulkiness and the flexibility of the dendra to be attached as a result of the high core branching multiplicity of ten or twelve. Indeed, in the case of the addition of the comparatively compact Fréchet-type G1 malonate **4**,[8] the resulting dendrimer **5** (Scheme 1) was obtained in only 2% yield. This yield was

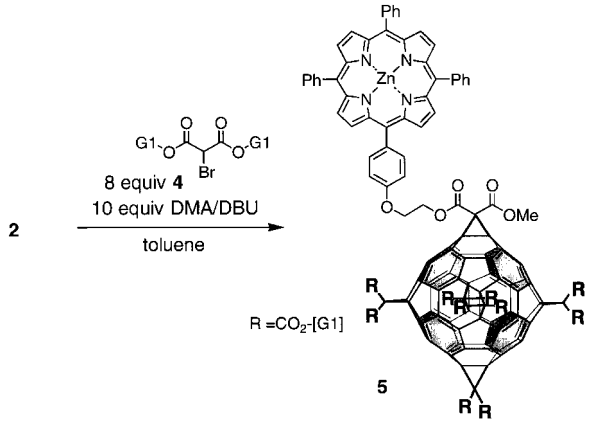

Scheme 1. Synthesis of the dendrimer–porphyrin–fullerene **5**.

obtained after repeated purification by flash chromatography followed by preparative HPLC on silica gel by using mixtures of toluene/ethyl acetate as eluents. Functional dendrimer **5** was characterized by NMR and UV/Vis spectroscopy as well as by mass spectrometry. The UV/Vis spectrum of the pink solution of **5** displays both the typical bands for the tetraphenylporphyrin (TPP) subunit, such as the Soret band at 413 nm and the Q bands at 548 and 586 nm, as well as the absorptions at 281, 311, and 345 nm characteristic of hexakis-adducts with a T_h-symmetric addition pattern. In the MALDI-TOF mass spectrum of **5**, the molecular ion peak at m/z 5093 appears as the only signal in the spectrum.

In order to avoid the problem of steric hindrance and to increase the yield of the convergently synthesized functional dendrimers, we developed a new type of dendra. For this purpose, we decided to introduce larger spacers, which should make the dendra more flexible and less densely packed. Our new modification of the classical Fréchet-type dendra contains a 3-oxypropane chain between the aryl–benzyl bond (Figure 2). Here, the typical aryl–benzyl sequence of the Fréchet dendra is transformed into an aryl–alkyl–benzyl

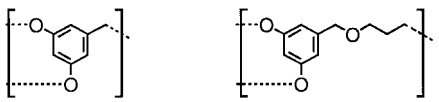

Figure 2. Schematic representation of a) Fréchet's dendra; b) a new dendritic system involving the introduction of a flexible spacer.

motif. The synthesis of the targets was planned according to the convergent approach developed by Fréchet and co-workers,[13] taking into account the concept of extended cores developed by Seebach and co-workers.[14, 15]

With this modification, two new additional steps per generation were added to the Fréchet route: the O-allylation of benzylic alcohols and the subsequent transformation of the allyl moiety into a terminal alcohol by means of hydroboration. The first- and second-generation dendritic alcohols were obtained according to the synthetic route shown in Scheme 2. Alcohol **6** was O-allylated by using sodium hydride as a base and a twofold excess of allyl bromide in refluxing THF to afford the allyl ether **7** in almost quantitative yield. Hydroboration of the allyl group in **7** with 9-borabicyclo[3.3.1]nonane (9-BBN) and subsequent oxidation of the intermediate borane with EtOH/NaOH/H_2O_2, furnished the corresponding first-generation alcohol **8** in 90% yield. The hydroboration was completely regioselective since no secondary alcohol was obtained. The conversion of **8** to bromide **9** with phosphorus tribromide provided a yield of only 12%, and the main product of the reaction was the bromide **10** (65%). Therefore, the synthesis of bromide **9** was carried out by treatment of the alcohol **8** with 1.3 equivalents of CBr_4/PPh_3 in THF.[9] In this case, the reaction worked satisfactorily, affording the desired bromide **9** in 94% yield. Selective alkylation of both phenolic hydroxyl groups of 3,5-dihydroxybenzyl alcohol **11** afforded the alcohol **12** in excellent yield. When the same sequence of O-allylation and oxidative hydroboration, described above, was applied to **12**, the second-generation alcohol **14** was formed as a pale yellow liquid. The purification of both intermediate **13** and product **14** was easily accomplished by flash chromatography on silica gel. The syntheses of these targets fulfil two important requirements desirable for dendrimer chemistry:

1) All transformations occur with high yields.
2) The isolation and the characterization of the consecutive dendritic wedges are both reliable and sensitive to the occurrence of impurities and defects.

The transformations of the first- and second-generation alcohols **8** and **14** into the malonates **15** and **17** were achieved by deprotonation with one equivalent of NaH in THF and subsequent reaction with malonyl dichloride (Scheme 3). The first-generation bromomalonate **16** was prepared by the reaction of **15** with CBr_4 in the presence of 1,8-diazobicyclo[5.4.0]undec-7-ene (DBU).[18]

The synthesis of the first-generation monoadduct **18** was straightforward, using classical Bingel reaction conditions (Scheme 4).[19] The product was isolated by flash chromatography on silica gel in 42% yield, together with unreacted C_{60} (23%) and a regioisomeric mixture of bisaddition products (15%).

0947-6539/99/0508-2364 $ 17.50+.50/0 *Chem. Eur. J.* **1999**, *5*, No. 8

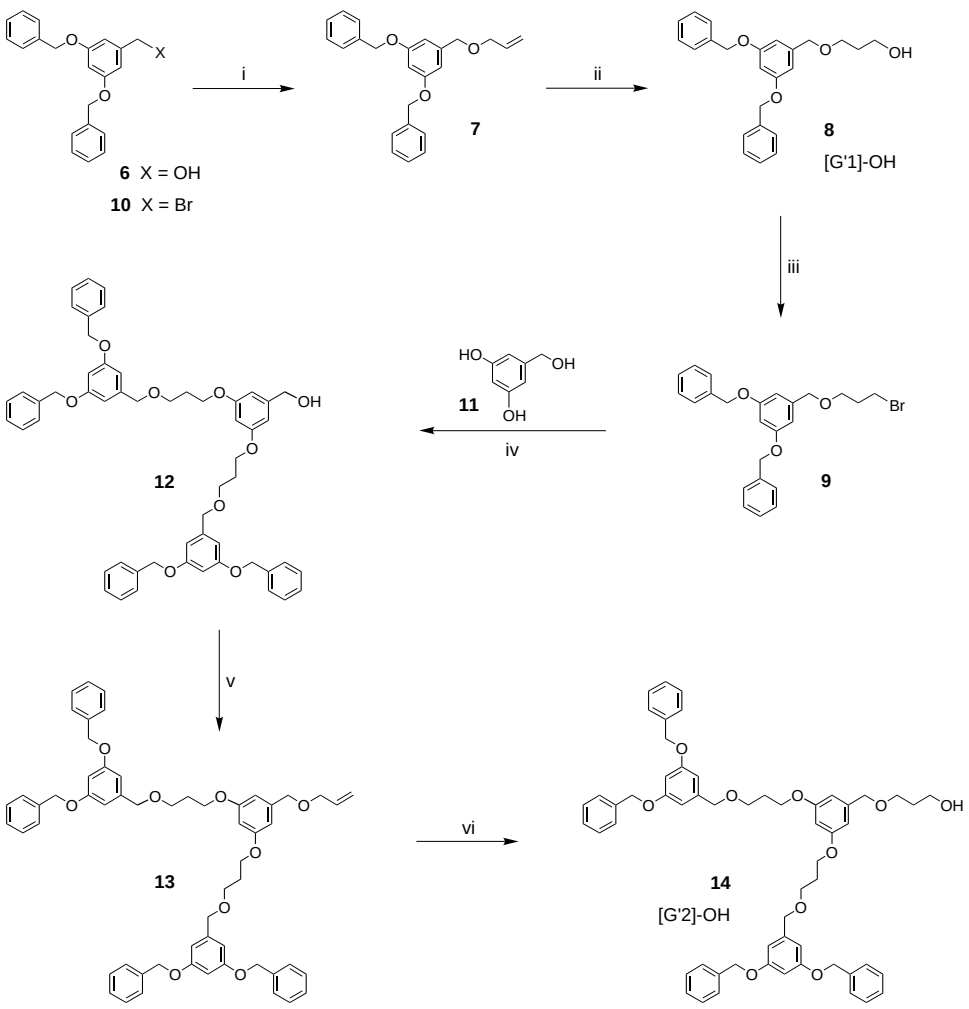

Scheme 2. Synthesis of dendritic polyether alcohols **8** and **14**. i) allyl bromide, NaH/THF (98%); ii) a) 9-BBN/THF; b) EtOH, H_2O_2, NaOH (90%); iii) CBr_4, PPh_3/THF (94%); iv) K_2CO_3, [18]crown-6/acetone (97%); v) allyl bromide, NaH/THF (97%); vi) a) 9-BBN–THF; b) EtOH, H_2O_2, NaOH (87%).

directly in a modified Bingel reaction that we developed previously.[20] The advantage of this method is the in situ generation of the reactive bromomalonic species, which allows the cyclopropanation of C_{60} starting directly from malonates. The treatment of C_{60} with equimolar amounts of **17** and CBr_4, and a little excess of DBU afforded monoadduct **19**, after purification with flash chromatography on silica gel in 42% yield (Scheme 4). The characterization of **18** and **19** using a variety of spectroscopic methods was straightforward. For example, ^{13}C NMR (Figure 3) and ^1H NMR spectra (Figure 4a) of **18**, as well as the NMR spectra of **19**, show all the expected peaks clearly resolved. The signals corresponding to the dendritic branches appear at about the same position as those on the precursor compounds **15** and **17**, respectively. The C atoms of the fullerene core appear at the typical positions for [6,6] bridged C_{60} monoadducts.[12] IR and UV/Vis spectra of **18** and **19** reveal the characteristic bands like the sharp monoadduct absorption at 426 nm.[12]

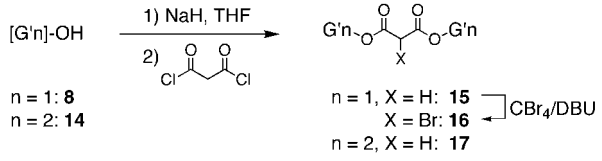

Scheme 3. Synthesis of the malonates **15**–**17**.

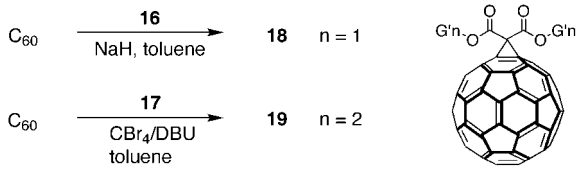

Scheme 4. Synthesis of the monoadducts **18** (first-generation) and **19** (second-generation).

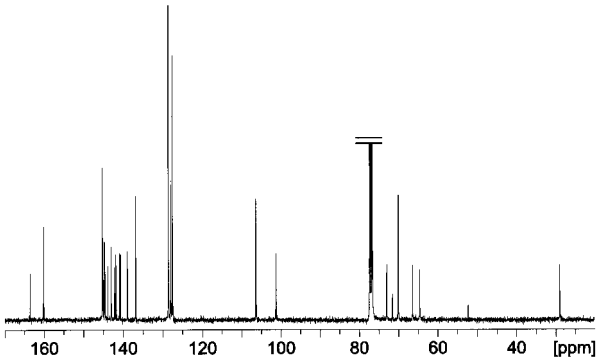

Figure 3. ^{13}C NMR spectrum (100.5 MHz, RT, $CDCl_3$) of **18**.

For the synthesis of the second-generation monoadduct **19**, malonate **17** was not further transformed into the corresponding bromomalonate as the reaction with C_{60} was carried out

The hexakisadduct **20** (Scheme 5) was synthesized by means of template activation with DMA as described above. The glassy yellow dendrimer **20** was isolated by using preparative HPLC on a silica column in 13% yield. The comparison with the yield of the hexakisadduct **1** without spacers[11] (5.4%) clearly shows that the modification of the dendrimer gives rise to reduced steric hindrance, which is usually involved in the synthesis of these crowded systems.

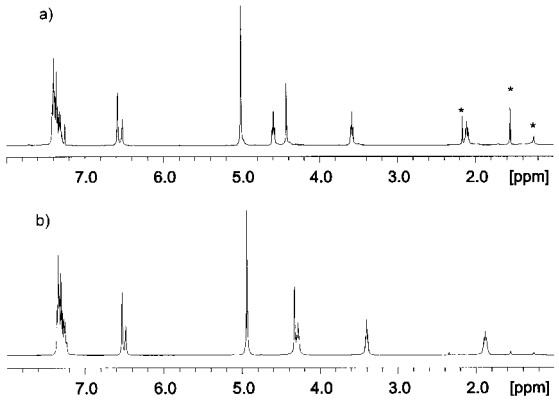

Figure 4. ^{1}H NMR spectra (400 MHz, RT, $CDCl_3$) of a) monoadduct **18** (*impurities), b) hexakisadduct **20**.

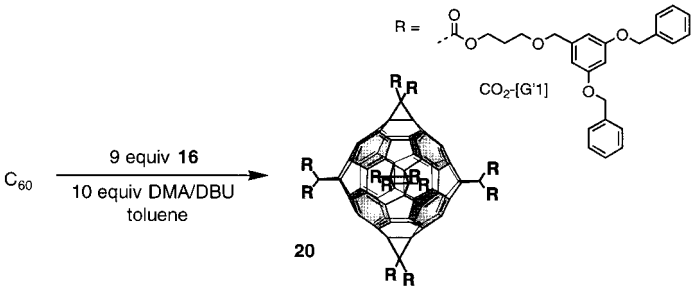

Scheme 5. Synthesis of the globular dendrimer hexakisadduct **20**.

Also, the purification was easier when the more flexible new dendra were used instead of the Fréchet type systems.

The ^{13}C NMR spectrum of **20** (Figure 5) clearly reveals the expected T_h symmetry, since only one set of signals for the dendra and the characteristic peaks of the three magnetically

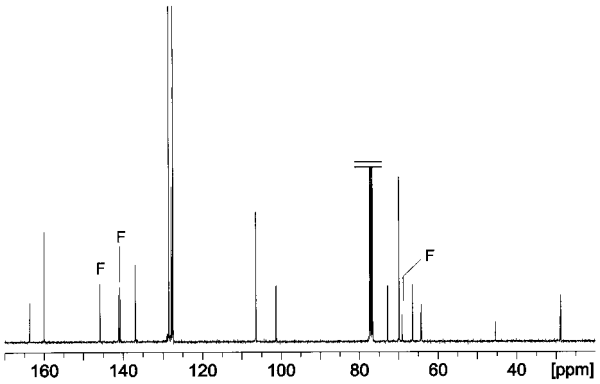

Figure 5. ^{13}C NMR spectrum (100.5 MHz, 31 °C, $CDCl_3$) of hexakisadduct **20**. F denotes the signals of the fullerene C atoms.

different C atoms of the fullerene core at $\delta = 145.89$, 141.22, and 69.14 appear. The ^{1}H NMR spectrum of **20** (Figure 4b) also confirms its high symmetry, since, as in the case of monoadduct **18**, just one set of signals for the protons of the addends appears. In contrast to the monoadduct **18** however, all the methylene protons of **20** are shifted to higher field. This effect was observed also for the dendrimer **1**[8] and is attributed to the interactions between the methylene protons and the ring currents of the comparatively densely packed aromatic rings within the macromolecule. The UV/Vis spectrum of **20** reveals the characteristic pattern of hexakis-adducts displaying a T_h-symmetrical addition pattern[11] with the main bands at $\lambda_{max} = 270$, 282, 320, 337, and 387 nm. MALDI-TOF mass spectrometry showing the molecular ion peak at 5658 amu confirmed the expected stoichiometry ($C_{366}H_{300}O_{60}$) of **20**.

The first- and second-generation functional dendrimers **21** and **22** were prepared analogously by means of template activation with DMA, but starting from porphyrin–fullerene dyad **2** (Scheme 6). Compound **21** was prepared by using

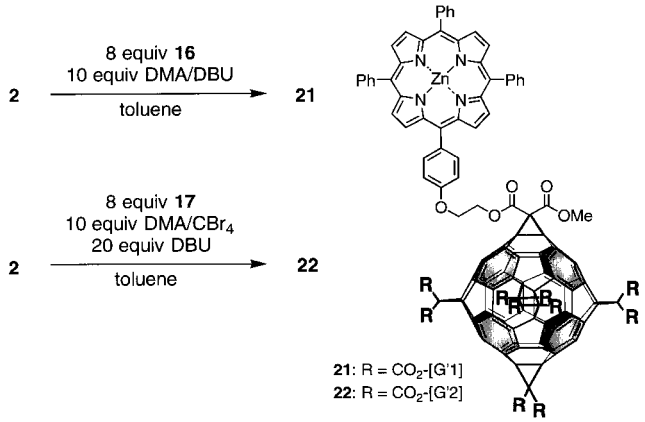

Scheme 6. Synthesis of the first- and second-generation functional dendrimers **21** and **22**.

bromomalonate **16**, whereas **22** was obtained directly from malonate **17** taking advantage of our modified Bingel reaction. The first-generation dendrimer **21** was isolated from the crude mixture in 12.7% yield using preparative HPLC. The characterization was carried out using ^{1}H NMR, ^{13}C NMR, IR, and UV/Vis spectroscopy as well as by mass spectrometry (Figure 6, Figure 7). Additional ^{1}H-^{13}C COSY NMR experiments enabled us to assign all peaks in the ^{13}C NMR and ^{1}H NMR spectra as shown in Figure 6. Although the symmetry of **21** is only C_s, the ^{13}C NMR spectrum is comparatively simple. Only a single set of peaks with resolved structure appears for the ten dendritic branches and three narrow distributions of peaks for the fullerene C atoms, two in the sp^2 and one in the sp^3 region. These results reflect the pseudo T_h-symmetrical addition pattern of **21**, resembling those of other mixed octahedrally coordinated hexakisadducts.[8, 10n, 11] Peaks corresponding to C atoms of the porphyrin appear at about the same position as in the monoadduct **2**.

The synthesis of **22** proved the success of the developed strategy. The introduction of the spacers into the dendra enabled the synthesis of a fullerene derivative containing ten second-generation dendra. The purification of this globular functional macromolecule required repeated chromatographic steps, resulting in the isolation of pure material in only 2% yield. The characterization of **22** was achieved by ^{1}H NMR, ^{13}C NMR, IR and UV/Vis spectroscopy (Figure 7). As a result of the higher molecular mass of 11078 amu and the larger number of magnetically inequivalent C atoms or protons, the

  0947-6539/99/0508-2366 $ 17.50+.50/0 *Chem. Eur. J.* **1999**, *5*, No. 8

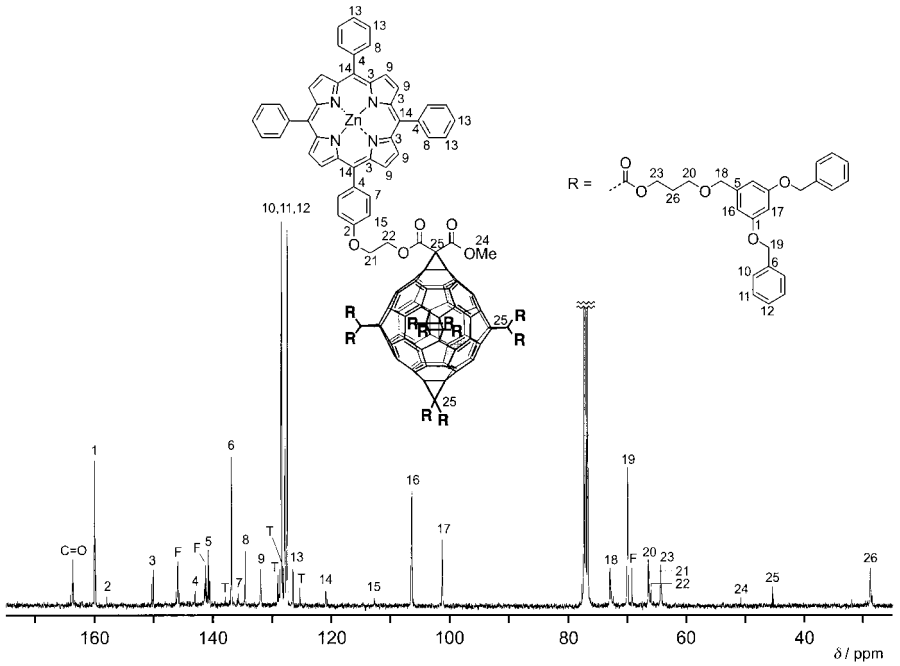

Figure 6. ^{13}C NMR (100.5 MHz, 31 °C, $CDCl_3$) spectrum of hexakisadduct **21**. F denotes the signals of the fullerene C atoms (T = toluene).

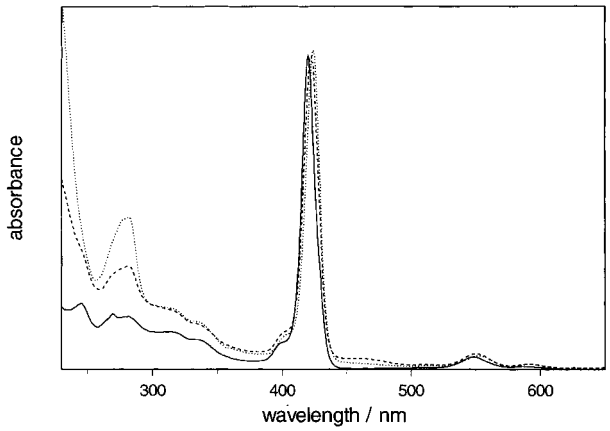

Figure 7. UV/Vis spectra (CH_2Cl_2) of the porphyrin–fullerene hexakisadduct **2** (solid line) and the porphyrin–dendrimer–fullerenes **21** (dashed line) and **22** (dotted line). The Soret bands are adjusted to the same absorbance.

NMR spectra are less resolved. However, as in the case of the NMR spectra of **21**, the pseudo T_h symmetry is still clearly reflected by the small number of signals for magnetically very similar nuclei of the addends and the fullerene core.

Comparison of the electronic absorption spectra of the dendrimers **21** and **22**, and hexakisadduct **3** reveals an influence of the nanoenvironment provided by the neighboring addends on the porphyrin chromophore (Figure 7). In the region between 230 and 380 nm, the absorptions of the fullerene core dominate the spectra. Adducts **3**, **21**, and **22** display bands at 270, 285, 315, and 335 nm, which are typical for hexakisadducts of C_{60} with a T_h-symmetrical addition pattern. As a result of the larger number of aromatic rings within the second-generation dendrimer **22**, the absorptions below 300 nm are stronger than those of the first-generation product **21**. From 380 nm, the spectra are dominated by the porphyrin chromophore, since the extinction coefficients of the fullerene core in this region are negligible compared to those of the porphyrin. Characteristic in this region are the Soret band at about 400 nm and the Q bands at about 550 and 590 nm. Relative to the dyad **2**, these porphyrin bands undergo a bathochromic shift of 4–7 nm for the second-generation system **22** and 2–4 nm for **21**. These shifts imply that the interaction between the porphyrin and the dendra increases with increasing generation number. In order to get an idea of the size and conformations of such macromolecular systems, we carried out a series of molecular modeling[21, 22] studies with the dendrimers **21** and **22.** The conformers obtained exhibit a globular structure, even for the first-generation adduct **21** (Figure 8). While in **21** the porphyrin chromophore still largely penetrates through the dendritic surrounding, in the second-generation representative **22**, it is partly covered. The calculated diameter of **22** is typically 5–6 nm.

The influence of the dendritic coverage in the functional dendrimers **21** and **22** on the redox potentials of the porphyrin and fullerene moieties was investigated. Cyclic voltammetric (CV) studies of compounds **2**, **3**, **21**, and **22** were performed.[23] These results are summarized in Table 1 (reduction) and Table 2 (oxidation). The complete assignment of the redox potentials was made on the basis of comparisons with model compounds: the porphyrin–malonate **23**,[10n] the monoadduct **24**,[19] and the hexakisadduct **25**.[11]

Table 1. $E_{1/2}$ [V] values measured as an average of the cathodic and anodic peak potentials. All values are based on the Fc/Fc^+ internal reference.

Compound	E_1	E_2	E_3	E_4
23	–1.88	–2.29*		
24	–1.06	–1.44	–1.89	
25	–1.69*	–2.35*		
2	–1.06	–1.44	–1.89	–2.05*
3	–1.69*	–2.13*	–2.32*	
21	–1.87	–2.15	–2.33	
22	–1.94*	–2.34*		

[*] Irreversible processes

Table 2. $E_{1/2}$ [V] values measured as an average of the anodic and cathodic peak potentials. All values are calculated based on the Fc/Fc^+ internal reference.

Compound	E_1	E_2
23	0.31	0.64
2	0.33	0.66
3	0.32	0.65
21	0.32	0.66

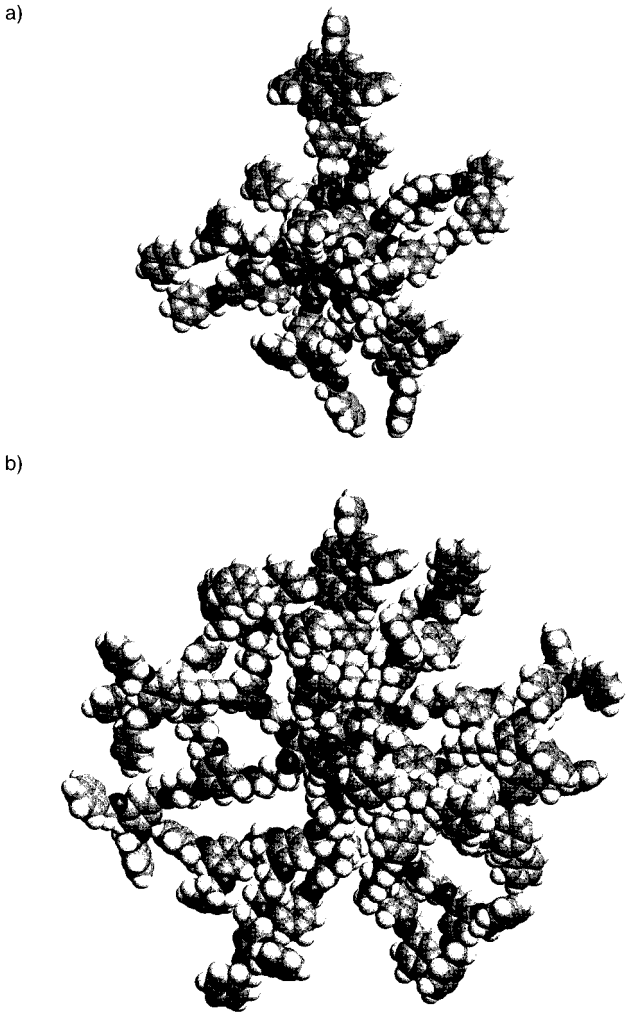

Figure 8. Optimized structures of the porphyrin–dendrimer–fullerenes a) **21** and b) **22**. All structures were minimized with the MM^+ force field implemented in HYPERCHEM.[22]

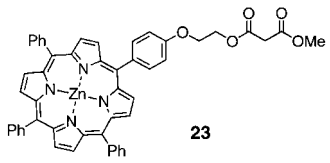

23

24

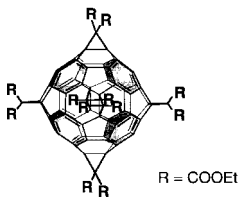

25

The cyclic voltammogram of **2** shows three reversible reductions with half-wave potentials equal to -1.06, -1.44, and -1.89 V (vs. Fc/Fc^+) based on the fullerene core (Figure 9, Table 1). These values are quite similar to those

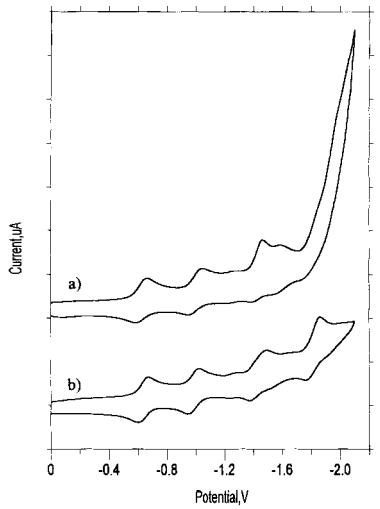

Figure 9. Cyclic voltammograms of **2** a) at room temperature and b) at low temperature ($-50\,^{\circ}C$). The experimental conditions were the same except for the temperature.

observed for the C_{60} monoadduct **24**. This is a clear indication that the attached porphyrin exerts essentially no influence on the electronic properties of the fullerene core.[10r, 24]

The fourth reduction of **2** is centered on the porphyrin portion, based on the result observed for the model porphyrin–malonate **23**. We also performed electrochemical experiments at low temperatures ($-50\,^{\circ}C$) with compound **2** (Figure 9b). The cathodic processes became significantly more reversible in these experiments. Similar improvements in the reversibility of fullerene derivative electrochemistry have been previously reported.[25] Compounds **3**, **21**, and **22** exhibit irreversible cathodic processes (Figure 10).

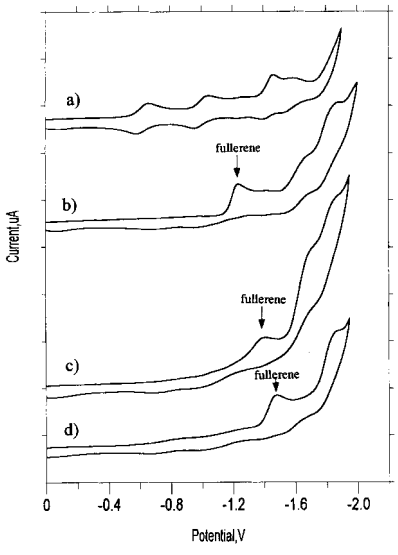

Figure 10. Cyclic voltammograms of compounds: a) **2**; b) **3**; c) **21**; and d) **22**. All experiments were performed under identical conditions with a scan rate of $100\,mV\,s^{-1}$. Ag/AgCl electrode was used as a reference electrode, and ferrocene was added as an internal reference.

0947-6539/99/0508-2368 $ 17.50+.50/0 *Chem. Eur. J.* **1999**, *5*, No. 8

In these cases, the high degree of addition on the fullerene cage disrupts the π system, making the reductions more difficult, as previously reported by others.[26] To gain further insight into the reasons for this, we carried out CV experiments on porphyrin–malonate **23** and hexakisadduct **25** under the same electrochemical conditions. The first reductions of **23**, **3**, and **25** are shown in Figure 11 with:

a) The reversible reduction peak of **23** ($E_{1/2} = -1.88$ V).
b) The irreversible reduction of **3** ($E_c = -1.69$ V).
c) The irreversible reduction of the hexakisadduct **25** ($E_c = -1.69$ V) (all values are vs. Fc/Fc^+).

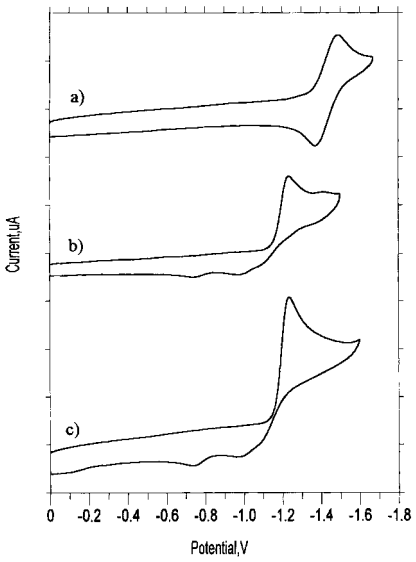

Figure 11. Cyclic voltammograms of compounds: a) **23**, b) **3**, and c) **25**. These were recorded under identical conditions with a scan rate of 100 $mV\,s^{-1}$, and ferrocene was added as an internal reference in all cases.

The resemblance (peak position and irreversible behavior) of the first reduction process for compounds **3** and the C_{60} hexakisadduct **25** is evident. Therefore, the first reduction observed for **3** can be safely assigned to a fullerene-based process. In analogy, the first reductions observed for **21** and **22** are also assigned to fullerene-based processes. It is interesting to note the pronounced and monotonic cathodic shift of this fullerene-based reduction with increasing dendrimer generation; the values range from −1.69 V for **3** to −1.87 V in compound **21**, to −1.94 V in compound **22**. As concluded from the comparison with model compounds,[10n] the next reduction of **3, 21**, and **22** is porphyrin-centered, but significantly cathodically shifted relative to **2**. The second porphyrin reduction is also cathodically shifted with increasing dendrimer generation; the values range from −2.13 V to −2.15 V, to −2.34 V, respectively. A third reduction process is observed in **3** and **21**. It is not possible to assign this process unequivocally, since based on the potential value and the potential gap it could be due to either the second reduction of the porphyrin or the fullerene.

The oxidations of compounds **2**, **3**, **21**, and **23** are listed in Table 2. The two oxidation potentials of each system are due to the zinc porphyrin. No significant shifts attributable to the nature of the addends can be detected. In each cyclic voltammogram, two weak additional peaks were observed, which are due to traces of metal-free porphyrin moieties. The oxidation potentials of the latter are more positive than those of the zinc–porphyrin group by ≈200 mV.[10c] The most crowded dendrimer **22** exhibits extremely small currents for the oxidation processes, and it is difficult to make definitive assignments of the anodic processes by cyclic voltammetry.

The fluorescence spectra of **2**, **3**, **21**, and **22** are shown in Figure 12. The presence of the malonate substituent causes a slight bathochromic shift of the fluorescence maximum at

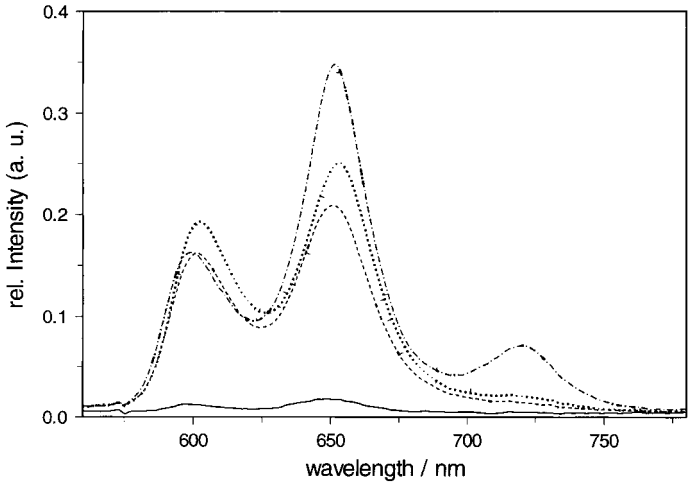

Figure 12. Fluorescence spectra of **2** (solid line), **3** (dash-dotted line), **21** (dashed line), and **22** (dotted line). The absorption at 720 nm in the spectrum of **3** is due to an impurity of the corresponding metal-free derivative.

650 nm of about 7 nm in comparison to that of Zn-TPP. The covalent binding of the C_{60} chromophore with and without additional malonate addends results in a bathochromic shift of the fluorescence maximum at 600 nm and a slight hypsochromic shift of the maximum at 650 nm. Altogether, the fluorescence of the TPP derivatives shows a bathochromic shift of 4–7 nm relative to that of the parent Zn-TPP. To control the purity of the different samples, the excitation spectra were measured (not shown). They fully reflect the absorption spectra and gave evidence of the presence of metal-free porphyrin in the sample **3**.

The fluorescence decay time of Zn-TPP (1.85 ns) is slightly reduced to 1.74 ns in the substituted porphyrin **23**. In the case of the dyad **2**, the intensity of the fluorescence bands is dramatically diminished, and the lifetime is decreased to a large extent to 0.22 ns at room temperature (Figure 12, Table 3). Since the C_{60} core is a good electron acceptor, the

Table 3. Singlet oxygen quantum yields (Φ_Δ) and fluorescence lifetimes (τ) of Zn-TPP, **2**, **3**, **21**, **22**, and **23**

Compound	τ [ns](±0.03)	Φ_Δ (±0.05)
Zn-TPP	1.85	0.78
23	1.74	0.76
2	0.22	0.45
3	1.74	0.73
21	1.77	0.66
22	1.77	0.67

shortened fluorescence decay time can be explained by an effective electron transfer[27] from the porphyrin to the fullerene chromophore. As already demonstrated with the electrochemical investigations, the addition of five dendritic or nondendritic malonates to give the hexakisadducts **3**, **21**, and **22** causes a dramatic decrease of the electron-accepting properties of the C_{60} core. As a consequence, electron transfer processes from the first excited singlet state (S_1) of the porphyrin to the C_{60} core, resulting in some contribution to the depopulation of S_1, do not occur. This explains the observed fluorescence decay times of 1.74 to 1.77 ns for the adducts **3**, **21**, and **22** (Table 3). These values are in good agreement with the decay time measured for **23** and confirm the assumption that no electron transfer occurs in these systems.

Electronically excited porphyrins[28] are known to generate molecular singlet oxygen ($^1\Delta_g$) by means of a highly efficient transfer of energy from their first excited triplet state (T_1) to molecular oxygen. It is also known that C_{60} has energy levels of the first excited singlet and triplet states,[29] which are comparable to those of extended π electron systems such as porphyrins, and that the values obtained for the intersystem crossing quantum yield are nearly one. Therefore, it was not surprising to determine a singlet oxygen quantum yield of 0.81 for parent C_{60}.[30] Owing to these properties of porphyrins and fullerenes, it was of interest to investigate the photosensitized $^1\Delta_g$ generation of the different samples and compare the results with those obtained for the S_1 state characterization.

For **23**, a singlet oxygen quantum yield of $\Phi_\Delta = 0.76$ was obtained (Table 3). This is nearly the same as that for Zn-TPP ($\Phi_\Delta = 0.78$). In the case of the hexakisadducts **3, 21**, and **22**, the singlet oxygen quantum yield is only slightly reduced to $\Phi_\Delta = 0.73$ for **3** and $\Phi_\Delta = 0.66$ and 0.67 for **21** and **22**, respectively. However, in the dyad **2**, Φ_Δ is only 0.45. This value is much higher than expected, considering our results obtained by dynamic fluorescence measurements. The behavior independently corroborates a photoinduced electron transfer from the porphyrin to the fullerene. This process could lead to the formation of the T_1 state of the C_{60} core,[31] from which in a second step $^1\Delta_g$ is generated. This assumption becomes plausible considering that the Φ_Δ of the parent C_{60} core is 0.81 and that of the porphyrin malonate **23** is 0.77 (Table 3). Further investigation to clarify the contributions of the different deactivation processes following the electronic excitation is currently underway.

Conclusion

The pronounced regioselectivity of template-mediated hexaadditions of malonates to octahedral [6,6] double bonds of C_{60} allows the facile synthesis of globular functional dendrimers with high core branching multiplicities involving a porphyrin chromophore. The electronic properties of the porphyrin moiety depend on the presence and the nature of the dendritic addends. The neighboring dendra determine the nanoenvironment of the porphyrin causing, for example, bathochromic shifts of the Soret and Q bands as well as shifts of the first reduction potential to more negative values with increasing generation number. Further systematic studies including the variation of the nature, the number, and the addition pattern of the attached dendra, the variation of the central metal of the porphyrin function as well as the investigation of the complexation behavior depending on the nanoenvironment of the metallomacrocycle, are being carried out in our laboratory in order to mimic the function of natural metalloproteins.

Experimental Section

^{1}H NMR and ^{13}C NMR spectroscopy: JEOL JNM EX 400 and JEOL JNM GX 400 (^{1}H NMR: 400 MHz; ^{13}C NMR: 100.5 MHz); MS: Varian MAT 311 A (EI), Finnigan MAT 900 (FAB); Micromass TofSpec (MALDI, α-cyano-4-hydroxycinnamic acid); FT-IR: Bruker Vector 22; UV/Vis: Shimadzu UV 3102 PC; HPLC preparative: Shimadzu SIL-10A, SPD-10A, CBM 10 A, LC 8 A, FRC 10A (Grom-Sil 100 Si, NP1, 5 μm, 250 × 20 mm); TLC (thin layer chromatography): Merck, silica gel 60 F_{254}. Reagents were commercially available reagent grade. Solvents were distilled and dried according to standard procedures. All reactions were carried out under a positive pressure of argon. Products were isolated where possible by flash column chromatography (silica gel 60, particle size 0.04 – 0.063 nm, Merck). 1′-Methoxycarbonyl-1′-[2-[4-[5-[10,15,20-triphenyl-porphyrinatozinc(II)]]phenoxy]ethoxycarbonyl]-1,2-methano[60]fullerene (**2**)[10n] and bromobis[(3,5-dibenzyloxy)benzyl]malonate (**4**)[8] were prepared as previously reported.

The absorption spectra were measured using a Shimadzu 160A spectral photometer. The experimental set-up for steady-state and time-resolved spectroscopic investigations has been described elsewhere.[32] Steady-state singlet oxygen measurements were carried out on a home-made piece of equipment, which has been described in ref. [33]. Time-resolved singlet oxygen luminescence detection was made using the apparatus described in ref. [34].

1,2-{[1′-Methoxycarbonyl-1′-[2-[4-[5-[10,15,20-triphenylporphyrinato-zinc(II)]]]-phenoxy]ethoxycarbonyl]methano}-18,36:22,23:27,45:31,32:55,-56-pentakis{bis[3,5-di(benzyloxy)benzyloxycarbonyl]methano}-1,2:18,36:-22,23:27,45:31,32:55,56-dodecahydro[60]fullerene (**5**): A solution of **2** (70 mg, 0.045 mmol) and DMA (96 mg, 0.46 mmol) in toluene (50 mL) was stirred at room temperature for 2 hours. Then **4** (284 mg, 0.361 mmol) and 1,8-diazabicyclo[5.4.0]undec-7-ene (DBU) (70 μL, 0.469 mmol) were added. After five days, the solvent was evaporated under reduced pressure, and the crude mixture was separated by flash chromatography (SiO_2, toluene/ethyl acetate 95:5), followed by preparative HPLC (SiO_2, toluene/ethyl acetate 95:5) to give **5** (5.1 mg, yield: 2.0 %).

^{1}H NMR (400 MHz, RT, $CDCl_3$): $\delta = 4.16$ (m, 2H; CH_2 porphyrin), 4.40 (m, 2H; CH_2 porphyrin), 4.63 (s, 23H; CH_2 dendrimer, CH_3 porphyrin), 4.89 (m, 40H; CH_2 dendrimer), 6.55 (m, 10H; dendrimer ArH), 6.62 (m, 20H; dendrimer ArH), 7.41 (m, 102H; dendrimer Ph, porphyrin Ph), 7.76 (m, 9H; porphyrin Ph), 8.13 (m, 2H; porphyrin Ph), 8.21 (m, 6H; porphyrin Ph), 8.93 (m, 8H; porphyrin β-pyrrole); UV/Vis (CH_2Cl_2): $\lambda_{max} = 271$, 281, 311 (sh), 345 (sh), 400 (sh), 419, 548, 587 nm; MS (MALDI-TOF): m/z: 5093 [M^+].

Allyl 3,5-(dibenzyloxy)benzyl ether (**7**): 3,5-(Dibenzyloxy)benzyl alcohol (**6**)[17] (31.23 g, 94.47 mmol) in THF (150 mL) was added to a slurry of NaH (7.8 g, 60 % in paraffin oil, 195 mmol) in THF (150 mL). The mixture was stirred under reflux for 30 min, then 3-bromoprop-1-ene (16.9 mL, 195 mmol) was added in one portion, and the mixture was refluxed for 24 h. Water was carefully added, the resulting mixture was extracted three times with Et_2O, the combined extract was dried over Na_2SO_4, and the solvent was evaporated under reduced pressure. Flash chromatography (SiO_2, hexanes/ethyl acetate 95:5) gave **7** (34.64 g, 98 %) as a colorless oil.

^{1}H NMR (400 MHz, RT, $CDCl_3$): $\delta = 4.99$ (dd, $J_1 = 6$ Hz, $J_2 = 1.6$ Hz, 2H; CH_2CH=), 4.45 (s, 2H; $ArCH_2O$), 5.01 (s, 4H; $PhCH_2O$), 5.17 – 5.21 (m, 1H; CHH=), 5.26 – 5.31 (m, 1H; CHH=), 5.88 – 5.99 (m, 1H; CH=CH_2), 6.54 (t, $J = 2$ Hz, 1H; ArH), 6.62 (d, $J = 2$ Hz, 2H; ArH), 7.29 – 7.42 (m, 10H; Ph); ^{13}C NMR (100.5 MHz, RT, $CDCl_3$): $\delta = 69.96$ ($PhCH_2$), 71.02 ($ArCH_2$), 71.89 (CH_2–CH=), 101.27, 106.49 (arom. CH), 117.17 (CH=CH_2), 127.54, 127.96, 128.56 (PhCH), 134.67 (CH=CH_2), 136.90 (PhC), 140.83, 160.07 (arom. C); MS (EI): m/z: 360 [M^+], 304, 181, 91; IR (film): $\tilde{\nu} = 3065$,

0947-6539/99/0508-2370 $ 17.50+.50/0 *Chem. Eur. J.* **1999**, *5*, No. 8

3033, 2925, 2861, 1586, 1498, 1452, 1376, 1293, 1158, 1059, 926, 832, 737, 697 cm^{-1}.

3-[3′,5′-Di(benzyloxy)benzyloxy]propanol (**8**): A 500 mL three-necked flask provided with addition funnel, argon inlet, reflux condenser, rubber septum, and stirring bar was charged with a solution (0.5 M) of 9-BBN in THF (100 mL, 50 mmol). Then a solution of **7** (16.64 g, 46.17 mmol) in THF (75 mL) was added dropwise at room temperature, and the resulting mixture was stirred for 14 h. The intermediate organoborane was oxidized by adding successively ethanol (3 mL), an aqueous solution of sodium hydroxide (6 M, 1 mL), and hydrogen peroxide (30 %, 2 mL) (10 times). The mixture was heated for 3 h at 50 °C and after that cooled to room temperature. The aqueous layer was saturated with potassium carbonate. Then the organic layer was separated, dried over Na_2SO_4, and the solvent was evaporated under reduced pressure. Flash chromatography (SiO_2, hexanes/ethyl acetate 3:2) yielded **8** (15.70 g, 90 %) as a colorless oil. ^{1}H NMR (400 MHz, RT, $CDCl_3$): $\delta = 1.81$ (tt, $J_1 = J_2 = 6$ Hz, 2H; CH_2), 2.45 (br, 1H; OH), 3.58 (t, $J = 6$ Hz, 2H; CH_2O), 3.72 (t, $J = 6$ Hz, 2H; CH_2OH), 4.42 (s, 2H; ArCH_2O), 4.99 (s, 4H; PhCH_2O), 6.53 (t, $J = 2$ Hz, 1H; ArH), 6.30 (d, $J = 2$ Hz, 2H; ArH), 7.27–7.41 (m, 10H; Ph); ^{13}C NMR (100.5 MHz, RT, $CDCl_3$): $\delta = 32.02$ (CH_2), 61.29 (CH_2OH), 69.86 (CH_2O), 69.89 (CH_2Ph), 72.92 (ArCH_2), 101.22, 106.37 (arom. CH), 127.46, 127.90, 128.50 (PhCH), 136.79 (PhC), 140.61, 160.03 (arom. C); MS (EI): *m/z*: 378 [M^+], 320, 304, 211, 181, 127, 91, 71; IR (film): $\tilde{\nu} = 3415$, 3089, 3064, 3033, 2928, 2870, 1596, 1498, 1453, 1375, 1293, 1214, 1157, 1059, 833, 738, 697 cm^{-1}.

3-Bromo-1-[3′,5′-di(benzyloxy)benzyloxy]propane (**9**): Triphenylphosphane (7.75 g, 29.60 mmol) was added to a solution of alcohol **8** (9.34 g, 24.67 mmol) and carbon tetrabromide (9.80 g, 29.55 mmol) in THF (150 mL). The mixture was stirred at room temperature under argon for 40 minutes. A TLC control showed the presence of starting alcohol **8** in the reaction mixture. Further portions of CBr_4 (0.818 g, 2.47 mmol) and PPh_3 (0.647 g, 2.47 mmol) were added, and the reaction mixture was stirred for another 40 minutes until TLC showed no trace of starting material. The reaction mixture was then poured into water and extracted with CH_2Cl_2. The combined extracts were dried with Na_2SO_4, filtered, and evaporated to dryness. Flash chromatography (SiO_2, hexanes/CH_2Cl_2 1:1) afforded **9** (10.26 g, 94 %) as a yellow oil. ^{1}H NMR (400 MHz, RT, $CDCl_3$): $\delta = 2.10$ (tt, $J_1 = J_2 = 6.4$ Hz, 2H; CH_2), 3.50 (t, $J = 6.4$ Hz, 2H; CH_2Br), 3.56 (t, $J = 6.4$ Hz, 2H; CH_2O), 4.44 (s, 2H; CH_2Ar), 5.03 (s, 4H; CH_2Ph), 6.55 (t, $J = 2.4$ Hz, 1H; ArH), 6.58 (d, $J = 2.4$ Hz, 2H; ArH), 7.29–7.43 (m, 10H; Ph); ^{13}C NMR (100.5 MHz, RT, $CDCl_3$): $\delta = 30.59$ (CH_2), 32.78 (CH_2Br), 67.61 (CH_2O), 70.00 (CH_2Ph), 72.92 (CH_2Ar), 101.30, 106.44 (arom. CH), 127.53, 127.99, 128.60 (PhCH), 136.90 (PhC), 140.77, 160.10 (arom. C); MS (EI): *m/z*: 442 [M^+], 304, 181, 91; IR (film): $\tilde{\nu} = 3089$, 3064, 3032, 2910, 2867, 1596, 1498, 1453, 1375, 1319, 1292, 1257, 1213, 1158, 1107, 1081, 1060, 1028, 832, 737, 697 cm^{-1}.

3,5-Bis[3′-[3″,5″-(dibenzyloxy)benzyloxy]propoxy]benzyl alcohol (**12**): A solution of 3,5-dihydroxybenzyl alcohol (1.71 g, 12.20 mmol), **9** (10.8 g, 24.47 mmol), dried potassium carbonate (4.215 g, 30.5 mmol), and [18]crown-6 (0.2 g, 0.76 mmol) in dry acetone (80 mL) was boiled stirring vigorously under nitrogen until no starting material or monoalkylated product was observed by TLC (72 h). The mixture was dried by using reduced pressure, the residue was divided between water and CH_2Cl_2, and the aqueous layer was extracted with CH_2Cl_2. The combined organic layers were dried over Na_2SO_4 and evaporated to dryness. Flash chromatography (SiO_2, hexanes/ethyl acetate 3:2) gave alcohol **12** (10.15 g, yield: 97 %). ^{1}H NMR (400 MHz, RT, $CDCl_3$): $\delta = 2.00$ (t, $J = 6$ Hz, 4H; CH_2), 2.10 (t, $J = 5$ Hz, 1H; −OH), 3.57 (t, $J = 6$ Hz, 4H; CH_2O), 3.98 (t, $J = 6$ Hz, 4H; CH_2), 4.40 (s, 4H; CH_2Ar), 4.44 (d, $J = 5$ Hz, 2H; CH_2OH), 4.93 (s, 8H; CH_2Ar), 6.37 (t, $J = 2.4$ Hz, 1H; ArH), 6.43 (d, $J = 2.4$ Hz, 2H; ArH), 6.51 (t, $J = 2.4$ Hz, 2H; ArH), 6.56 (d, $J = 2.4$ Hz, 4H; ArH), 7.24–7.37 (m, 20H; Ph); ^{13}C NMR (100.5 MHz, RT, $CDCl_3$): $\delta = 29.46$ (CH_2), 64.62, 64.87, 66.62 (CH_2O), 69.80 (CH_2Ph), 72.70 (CH_2Ar), 100.34, 101.15, 104.95, 106.32 (arom. CH), 127.43, 127.84, 128.44 (PhCH), 136.78 (PhC), 140.84, 143.41, 159.93, 160.21 (arom. C); MS (FAB): *m/z*: 860 [M^+]; IR (film): $\tilde{\nu} = 3448$, 3089, 3064, 3032, 2931, 2871, 1596, 1498, 1453, 1376, 1319, 1293, 1215, 1160, 1104, 1082, 1060, 833, 738, 697 cm^{-1}.

Allyl 3,5-bis[3′-[3″,5″-(dibenzyloxy)benzyloxy]propoxy]benzyl ether (**13**): In a similar procedure to that described for **7**, the reaction was performed using compound **12** (10.05 g, 11.67 mmol), NaH (0.8 g, 60 % in paraffin oil, 20 mmol), and allyl bromide (17.5 mL, 20 mmol) in THF (100 mL). Flash chromatography (SiO_2, hexanes/ethyl acetate 4:1) yielded **13** (10.06 g, 96 %). ^{1}H NMR (400 MHz, RT, $CDCl_3$): $\delta = 2.02$ (tt, $J_1 = J_2 = 6$ Hz, 4H; CH_2), 3.59 (t, $J = 6$ Hz, 4H; CH_2OCH_2), 3.96 (ddd, $J_1 = 5.6$ Hz, $J_2 = J_3 = 1.6$ Hz, 2H; CH_2−CH=), 4.38 (s, 2H; CH_2Ar), 4.23 (s, 4H; CH_2Ar), 4.97 (s, 8H; CH_2Ar), 5.17 (dtd, $J_1 = 10.0$ Hz, $J_2 = J_3 = 1.6$ Hz, 1H; C*H*H=), 5.28 (dtd, $J_1 = 17.6$ Hz, $J_2 = J_3 = 1.6$ Hz, 1H; C*H*H=), 5.91 (ddt, $J_1 = 17.6$ Hz, $J_2 = 10$ Hz, $J_3 = 5.6$ Hz, 1H; C*H*=CH_2), 6.39 (t, $J = 2$ Hz, 1H; ArH), 6.48 (d, $J = 2$ Hz, 2H; ArH), 6.52 (t, $J = 2$ Hz, 2H; ArH), 6.58 (d, $J = 2$ Hz, 4H; ArH), 7.26–7.39 (m, 20H; Ph); ^{13}C NMR (100.5 MHz, RT, $CDCl_3$): $\delta = 29.55$ (CH_2), 64.70, 66.75, 69.86, 70.96, 71.87, 72.79 (CH_2O), 100.51, 101.21, 105.87, 106.32 (arom. CH), 117.01 (CH_2=CH−), 127.46, 127.88, 128.49 (PhCH), 134.69 (CH_2=C*H*−), 136.86 (PhC), 140.65 (CH_2=*C*H−), 140.92, 160.01, 160.22 (arom. C); MS (EI): *m/z*: 900 [M^+], 303, 213, 181, 163, 123, 91, 65; IR (film): $\tilde{\nu} = 3088$, 3064, 3033, 2931, 2867, 1596, 1498, 1453, 1376, 1320, 1293, 1215, 1160, 1102, 1061, 929, 833, 737, 697 cm^{-1}.

3-{3′,5′-Bis[3″-[bis(3‴,5‴-dibenzyloxy)benzyl]propoxy]benzyloxy}propanol (**14**): According to the same procedure described for **8**, the reaction was performed starting with allyl ether **13** (9.12 g, 10.12 mmol) dissolved in THF (100 mL) and 9-BBN (0.5 M, 23 mL, 11.5 mmol). After the oxidation step, the crude mixture was purified by flash chromatography (SiO_2, hexanes/ethyl acetate 3:2) to furnish **14** (8.09 g, 87 %). ^{1}H NMR (400 MHz, RT, $CDCl_3$): $\delta = 1.81$ (tt, $J_1 = J_2 = 6$ Hz, 2H; CH_2), 2.03 (tt, $J_1 = J_2 = 6$ Hz, 4H; CH_2), 2.30 (br s, 1H; OH), 3.58 (t, $J = 6$ Hz, 2H; CH_2OH), 3.60 (t, $J = 6$ Hz, 4H; CH_2O), 3.73 (t, $J = 6$ Hz, 2H; CH_2O), 4.02 (t, $J = 6$ Hz, 4H; CH_2OAr), 4.37 (s, 2H; CH_2Ar), 4.44 (s, 4H; CH_2Ar), 4.98 (s, 8H; CH_2Ph), 6.38 (t, $J = 2$ Hz, 1H; ArH), 6.45 (d, $J = 2$ Hz, 2H; ArH), 6.53 (t, $J = 2.4$ Hz, 2H; ArH), 6.58 (d, $J = 2.4$ Hz, 4H; ArH), 7.27–7.40 (m, 20H; Ph); ^{13}C NMR (100.5 MHz, RT, $CDCl_3$): $\delta = 29.54$, 31.98 (CH_2), 61.57 (CH_2OH), 64.72 (CH_2OAr), 66.77, 69.04 (CH_2OCH_2), 69.90 (CH_2Ph), 72.81, 73.00 (CH_2Ar), 100.52, 101.20, 105.82, 106.36 (arom. CH), 127.51, 127.92, 128.52 (PhCH), 136.86 (PhC), 140.46, 140.91, 160.02, 160.27 (arom. C); MS (EI): *m/z*: 918 [M^+], 91, 65, 43; IR (film): $\tilde{\nu} = 3462$, 3088, 3064, 3032, 3008, 2930, 2868, 1598, 1498, 1453, 1375, 1319, 1293, 1215, 1150, 1102, 1082, 1059, 832, 737, 697 cm^{-1}.

Bis{3-[3′,5′-di(benzyloxy)benzyloxy]propyl}malonate (**15**): To a slurry of NaH (450 mg, 60 % in paraffin-oil, 11.25 mmol) in dry THF (20 mL), compound **8** (4.05 g, 10.70 mmol) in dry THF (50 mL) was added. The mixture was stirred at room temperature for 45 min and then added using a double-ended needle to another flask, which contained malonyl dichloride (0.51 mL, 5.24 mmol) in dry THF (20 mL). The resulting mixture was stirred for 3 h at room temperature. After that HCl (0.1 M, 100 mL) was carefully added, and the resulting mixture was extracted three times with Et_2O. The combined extract was washed with a saturated solution of $NaHSO_4$, dried over Na_2SO_4, and the solvent evaporated under reduced pressure. Flash chromatography (SiO_2, hexanes/ethyl acetate 3:1) gave **15** (4.03 g, 93 %) as an oil. ^{1}H NMR (400 MHz, RT, $CDCl_3$): $\delta = 1.92$ (tt, $J_1 = J_2 = 6$ Hz, 4H; CH_2), 3.34 (s, 2H; CH_2), 3.50 (t, $J = 6$ Hz, 4H; CH_2O), 4.25 (t, $J = 6$ Hz, 4H; CH_2OOC), 4.42 (s, 4H; ArCH_2O), 5.02 (s, 8H; PhCH_2O), 6.54 (t, $J = 2$ Hz, 2H; ArH), 6.57 (d, $J = 2$ Hz, 4H; ArH), 7.29–7.43 (m, 20H; Ph); ^{13}C NMR (100.5 MHz, RT, $CDCl_3$): $\delta = 28.83$, 41.46, 62.71, 66.42, 70.02, 72.88 (CH_2), 101.27, 106.48 (arom. CH), 127.58, 128.01, 128.61 (PhCH), 136.92 (PhC), 140.82, 160.12 (arom. C), 166.62 (C=O); MS (EI): *m/z*: 824 [M^+], 644, 577, 492, 446, 378, 304, 211, 181; IR (film): $\tilde{\nu} = 3089$, 3064, 3033, 2930, 2868, 1734, 1596, 1498, 1454, 1375, 1331, 1293, 1244, 1158, 1108, 1086, 833, 739, 698 cm^{-1}.

Bromo bis{3-[3′,5′-di(benzyloxy)benzyloxy]propyl}malonate (**16**): A mixture of malonate **15** (3.8 g, 4.606 mmol) and DBU (0.69 mL, 4.618 mmol) in THF (30 mL) was cooled to −78 °C under argon. A solution of CBr_4 (1.53 g, 4.613 mmol) in THF (30 mL) was added, and the mixture was stirred for two hours. The reaction was quenched with HCl (0.1 M, 50 mL), and the cooling bath was removed. Et_2O was added, the organic layer was extracted with saturated aqueous $NaHCO_3$ (to pH 6) and saturated NaCl solutions, and was dried over Na_2SO_4. Flash chromatography (SiO_2, hexanes/ethyl acetate 3:1) gave **16** (3.02 g, 73 %) as a yellow oil. ^{1}H NMR (400 MHz, RT, $CDCl_3$): $\delta = 1.88$ (tt, $J_1 = J_2 = 6$ Hz, 4H; CH_2), 3.48 (t, $J = 6$ Hz, 4H; CH_2O), 4.31 (t, $J = 6$ Hz, 4H; CH_2OOC), 4.40 (s, 4H; ArCH_2O), 4.81 (s, 1H; CHBr), 5.00 (s, 8H; PhCH_2O), 6.54 (t, $J = 2$ Hz, 2H; ArH), 6.56 (d, $J = 2$ Hz, 4H; ArH), 7.27–7.41 (m, 20H; Ph); ^{13}C NMR (100.5 MHz, RT, $CDCl_3$): $\delta = 28.61$ (CH_2), 42.06 (CHBr), 64.21, 66.00, 69.91, 72.81 (CH_2), 101.22, 106.49 (arom. CH), 127.47, 127.90, 128.51 (PhCH), 136.84 (PhC), 140.66, 160.04 (arom. C), 164.51 (C=O); MS (EI): *m/z*: 904 [M^+],

824, 664, 586, 304, 181, 91; IR (film): $\tilde{\nu}$ = 3089, 3064, 3032, 2960, 2927, 2868, 1742, 1596, 1498, 1453, 1376, 1294, 1157, 1108, 1059, 909, 833, 738, 697 cm^{-1}.

Bis-3-{3′,5′-bis[3″-[bis(3‴,5‴-dibenzyloxy)benzyl]propoxy]benzyloxy}propylmalonate (**17**): According to the same procedure described for **15**, the reaction was carried out with **14** (5.02 g, 5.46 mmol) and NaH (220 mg 60% in paraffin-oil, 5.50 mmol) in THF (30 mL), and malonyl dichloride (0.265 mL, 2.72 mmol) in THF (20 mL). Flash chromatography (SiO_2, hexanes/ethyl acetate 3:1) gave **17** (2.39 g, yield: 46%) as a dense oil. ^{1}H NMR (400 MHz, RT, $CDCl_3$): δ = 1.90 (tt, $J_1 = J_2 = 6$ Hz, 4H; CH_2), 2.02 (tt, $J_1 = J_2 = 6$ Hz, 8H; CH_2), 3.31 (s, 2H; $COCH_2CO$), 3.46 (t, $J = 6$ Hz, 4H; CH_2OCH_2), 3.59 (t, $J = 6$ Hz, 8H; CH_2OCH_2), 4.01 (t, $J = 6$ Hz, 8H; CH_2OAr), 4.23 (t, $J = 6$ Hz, 4H; CH_2OOC), 4.35 (s, 4H; CH_2Ar), 4.24 (s, 8H; CH_2Ar), 4.96 (s, 16H; CH_2Ph), 6.38 (t, $J = 2.4$ Hz, 2H; ArH), 6.45 (d, $J = 2.4$ Hz, 4H; ArH), 6.52 (t, $J = 2.4$ Hz, 4H; ArH), 6.57 (d, $J = 2.4$ Hz, 8H; ArH), 7.25 – 7.40 (m, 40H; Ph); ^{13}C NMR (100.5 MHz, RT, $CDCl_3$): δ = 28.70, 29.52, 41.26 (CH_2), 62.61 (CH_2OOC), 64.67 (CH_2OAr), 66.31 (CH_2OCH_2), 66.73 (CH_2OCH_2), 69.83 (CH_2Ph), 72.75 (2 × CH_2Ar), 100.37, 101.16, 105.80, 106.30 (arom. CH), 127.44, 127.85, 128.46 (PhCH), 136.83 (PhC), 140.58, 140.91, 159.97, 160.20 (arom. C), 166.47 (C=O); MS (FAB): m/z: 2039 [M+Cs$^+$], 1906 [M^+]; IR (film): $\tilde{\nu}$ = 3089, 3064, 3033, 2930, 2868, 1750, 1733, 1596, 1498, 1453, 1376, 1293, 1215, 1158, 1105, 1060, 910, 832, 738, 697, 666 cm^{-1}.

1,2-Bis{3-[3′,5′-di(benzyloxy)benzyloxy]propoxycarbonyl}methano-1,2-dihydro-[60]fullerene (**18**): To a solution of C_{60} (62 mg, 0.086 mmol) and bromomalonate **16** (110 mg, 0.122 mmol) in toluene (60 mL), sodium hydride (20 mg, 0.833 mmol) was added. After stirring the mixture for 72 h at room temperature, the excess NaH was neutralized with H_2SO_4 (2N). The organic layer was dried over $MgSO_4$, and the solvent evaporated under reduced pressure. Flash chromatography (SiO_2, toluene/ethyl acetate 98:2) afforded C_{60} (23 mg, 37%), **18** (55 mg, 41%), and a mixture of the corresponding bisadducts (31 mg, yield: 15%). ^{1}H NMR (400 MHz, RT, $CDCl_3$): δ = 2.11 (tt, $J_1 = J_2 = 6$ Hz, 4H; CH_2), 3.59 (t, $J = 6$ Hz, 4H; CH_2O), 4.58 (t, $J = 6$ Hz, 4H; CH_2OOC), 4.61 (s, 4H; $ArCH_2O$), 5.01 (s, 8H; $PhCH_2O$), 6.52 (t, $J = 2$ Hz, 2H; ArH), 6.58 (d, $J = 2$ Hz, 4H; ArH), 7.29 – 7.42 (m, 20H; Ph); ^{13}C NMR (100.5 MHz, RT, $CDCl_3$): δ = 28.97 (CH_2), 52.28 (methano bridge), 64.57, 66.39, 70.03 (CH_2), 71.54 (C_{60} sp^3 C), 73.02 (CH_2), 101.30, 106.43 (arom. CH), 127.61, 128.03, 128.62 (PhCH), 136.89 (PhC), 138.98 (C_{60} sp^2 C), 140.72 (arom. C), 140.97, 141.89, 142.23, 143.02, 143.05, 143.90, 144.63, 144.66, 144.73, 144.93, 145.13, 145.23, 145.29 (C_{60} sp^2 C), 160.16 (arom. C), 163.65 (C=O); UV/Vis (CH_2Cl_2): λ_{max} = 259, 328, 426, 485 nm; MS (MALDI-TOF): m/z: 1543 [M^+]; IR (KBr): $\tilde{\nu}$ = 3088, 3062, 3029, 2955, 2924, 2857, 1744, 1594, 1497, 1452, 1375, 1292, 1267, 1233, 1155, 1106, 1059, 830, 736, 696, 526 cm^{-1}.

1,2-Bis{3-[3′,5′-bis[3″-[bis(3‴,5‴-dibenzyloxy)benzyl]propoxy]benzyloxy}propoxy-oxycarbonyl}methano-1,2-dihydro-[60]fullerene (**19**): To a mixture of C_{60} (36 mg, 0.050 mmol), CBr_4 (17 mg, 0.051 mmol), and malonate **17** (95 mg, 0.051 mmol) in toluene (40 mL), DBU (9 μL, 0.060 mmol) was added. After 24 hours, the solvent was removed under reduced pressure, and the crude mixture was separated by flash chromatography (SiO_2, toluene increasing to toluene/ethyl acetate 9:1) to yield [60]fullerene monoadduct **19** (55 mg, yield: 42%). ^{1}H NMR (400 MHz, RT, $CDCl_3$): δ = 2.02 (tt, $J_1 = J_2 = 6$ Hz, 8H; CH_2), 2.10 (tt, $J_1 = J_2 = 6$ Hz 4H; CH_2), 3.56 (t, $J = 6$ Hz, 4H; CH_2OCH_2), 3.59 (t, $J = 6$ Hz, 8H; CH_2OCH_2), 4.01 (t, $J = 6$ Hz, 8H; CH_2OAr), 4.36 (s, 4H; CH_2Ar), 4.43 (s, 8H; CH_2Ar), 4.58 (t, $J = 6$ Hz, 4H; CH_2OOC), 4.98 (s, 16H; CH_2Ph), 6.36 (t, $J = 2$ Hz, 2H; ArH), 6.44 (d, $J = 2$ Hz, 4H; ArH), 6.52 (t, $J = 2.4$ Hz, 4H; ArH), 6.57 (d, $J = 2.4$ Hz, 8H; ArH), 7.23 – 7.40 (m, 40H; Ph); ^{13}C NMR (100.5 MHz, RT, $CDCl_3$): δ = 28.92, 29.63 (CH_2), 52.30 (methano bridge), 64.56 (CH_2COO), 64.80 (CH_2OAr), 66.37, 66.90 (CH_2OCH_2), 69.97 (CH_2Ph), 71.50 (C_{60} sp^3 C), 72.87, 73.05 (CH_2Ar), 100.52, 101.23, 105.97, 106.39 (arom. CH), 127.57, 127.98, 128.58 (PhCH), 136.90 (PhC), 140.53 (arom. C), 140.92 (C_{60} sp^2 C), 140.99 (arom. C), 141.84, 142.16, 142.96, 142.99, 143.84, 144.57, 144.60, 144.67, 144.87, 145.07, 145.16, 145.22, 145.26 (C_{60} sp^2 C), 160.08, 160.13 (arom. C), 163.61 (C=O); UV/Vis (CH_2Cl_2): λ_{max} = 260, 327, 426, 490 nm; MS (FAB): m/z: 2756 [M+Cs$^+$]; IR (film): $\tilde{\nu}$ = 3087, 3062, 3030, 2925, 2861, 1744, 1595, 1497, 1451, 1374, 1292, 1234, 1158, 1104, 1059, 831, 737, 697, 527 cm^{-1}.

1,2:18,36:22,23:27,45:31,32:55,56-Hexakis{bis{3-[3′,5′-di(benzyloxy)benzyloxy]propoxy-carbonyl}methano}-1,2:18,36:22,23:27,45:31,32:55,56-dodecahydro[60]fullerene (**20**): A mixture of C_{60} (130 mg, 0.180 mmol) and DMA (370 mg, 1.80 mmol) in toluene (90 mL) was stirred at room temperature for 2 hours. Then bromomalonate **16** (1.5 g, 1.67 mmol) and DBU (0.276 mL, 1.85 mmol) were added. After 72 h, the crude mixture was separated first by flash chromatography (SiO_2, toluene/ethyl acetate 98:2 increasing to 9:1) followed by preparative HPLC (SiO_2, toluene/ethyl acetate 95:5) to afford hexakisadduct **20** (130 mg, yield: 13%) as a yellow glass.

^{1}H NMR (400 MHz, RT, $CDCl_3$): δ = 1.88 (tt, $J_1 = J_2 = 6$ Hz, 24H; CH_2), 3.40 (t, $J = 6$ Hz, 24H; CH_2O), 4.28 (t, $J = 6$ Hz, 24H; CH_2OOC), 4.33 (s, 24H; $ArCH_2O$), 5.94 (s, 48H; $PhCH_2O$), 6.48 (t, $J = 2$ Hz, 12H; ArH), 6.53 (d, $J = 2$ Hz, 24H; ArH), 7.22 – 7.36 (m, 120H; Ph); ^{13}C NMR (100.5 MHz, RT, $CDCl_3$): δ = 28.78 (CH_2), 45.37 (methano bridge), 64.27, 66.41 (CH_2), 69.14 (C_{60} sp^3 C), 69.90, 72.84 (CH_2), 101.27, 106.41 (arom. CH), 127.51, 127.89, 128.53 (PhCH), 136.93 (PhC), 140.81 (arom. C), 141.22, 145.89 (C_{60} sp^2 C), 160.03 (arom. C), 163.69 (C=O); UV/Vis (CH_2Cl_2): λ_{max} = 270, 282, 320, 337, 387 nm; MS (MALDI-TOF): m/z: 5681 [M+Na$^+$), 5658 [M^+]; IR (KBr): $\tilde{\nu}$ = 3088, 3063, 3031, 3007, 2956, 2924, 2865, 1744, 1595, 1497, 1453, 1375, 1292, 1265, 1215, 1156, 1107, 1080, 1059, 831, 737, 714, 697, 528 cm^{-1}.

1,2-{[1′-Methoxycarbonyl-1′-[2-[4-[5-[10,15,20-triphenylporphyrinatozinc(II)]]]-phenoxy]ethoxycarbonyl]methano}-18,36:22,23:27,45:31,32:55,56-pentakis{bis{3-[3′,5′-di(benzyloxy)benzyloxy]propoxycarbonyl}methano}-1,2:18,36:22,23:27,45:31,32:55,56-dodecahydro[60]fullerene (**21**): A mixture of **2** (100 mg, 0.064 mmol) and DMA (120 mg, 0.578 mmol) in toluene (50 mL) was stirred at room temperature for 2 h. Then bromomalonate **16** (523 mg, 0.578 mmol) in toluene (10 mL) and DBU (86 μL, 0.578 mmol) were added. After four days the solvent was evaporated under reduced pressure, and the crude mixture separated by flash chromatography (SiO_2, toluene increasing to toluene/ethyl acetate 95:5) followed by preparative HPLC (SiO_2, toluene/ethyl acetate 95:5) to give the porphyrin-dendrimer – [60]fullerene **21** (47 mg, 13%).

^{1}H NMR (400 MHz, RT, $CDCl_3$): δ = 1.72 – 1.92 (m, 20H; dendrimer CH_2), 3.31 – 3.41 (m, 20H; dendrimer CH_2), 4.13 (s, 3H; CH_3), 4.24 – 4.34 (m, 42H; CH_2 dendrimer, CH_2 porphyrin), 4.68 (br, 2H; CH_2 porphyrin), 4.82 – 4.94 (m, 40H; CH_2 dendrimer), 6.30 – 6.53 (m, 30H; dendrimer ArH), 7.16 – 7.35 (m, 102H; dendrimer Ph, porphyrin Ph), 7.68 – 7.72 (m, 9H; porphyrin Ph), 8.09 (m, 2H; porphyrin Ph), 8.17 (m, 6H; porphyrin Ph), 8.88 – 8.90 (m, 8H; porphyrin β-pyrrole); ^{13}C NMR (100.5 MHz, RT, $CDCl_3$): δ = 28.52, 28.85 (CH_2), 45.20, 45.46 (methano bridge), 50.77 (CH_3O), 64.30, 65.98, 66.31, 66.42 (CH_2O), 69.18 (C_{60} sp^3 C), 69.93, 72.87 (CH_2O), 101.23, 106.25, 106.39, 112.70 (arom. CH), 120.81, 120.90 (porphyrin C), 126.47, 127.47, 127.85, 128.49 (PhCH), 131.87, 131.96 (β-pyrrole CH), 134.48, 135.61 (PhCH), 136.76, 136.79, 136.85 (PhC), 140.42, 140.56, 140.69, 140.74, 140.92 (arom. C), 141.10, 141.19, 141.31 (C_{60} sp^2 C), 142.97 (β-pyrrole C), 145.64, 145.87, 145.94, 146.13 (C_{60} sp^2 C), 150.03, 150.33 (PhC), 157.87, 159.82, 159.91, 159.95 (arom. C), 163.61, 164.14 (C=O); UV/Vis (CH_2Cl_2): λ_{max} = 271, 283, 315 (sh), 338 (sh), 400 (sh), 422, 551, 591 nm; MS (MALDI-TOF): m/z: 5669 [M^+]; 4844 [$M - C_{51}H_{50}O_{10}^+$]; IR (KBr): $\tilde{\nu}$ = 3061, 3030, 2924, 2863, 1744, 1595, 1452, 1375, 1264, 1215, 1154, 1059, 830, 736, 697, 528 cm^{-1}.

1,2-{[1′-Methoxycarbonyl-1′-[2-[4-[5-[10,15,20-triphenylporphyrinatozinc(II)]]]-phenoxy]ethoxycarbonyl]methano}-18,36:22,23:27,45:31,32:55,56-pentakis{bis{3-[3′,5′-bis[3″-[bis(3‴,5‴-dibenzyloxy)benzyl]propoxy]benzyloxy}propoxycarbonyl}methano}-1,2:18,36:22,23:27,45:31,32:55,56-dodecahydro[60]fullerene (**22**): According to the preparation of **21**, the reaction was performed with **1** (90 mg, 0.0578 mmol), DMA (107 mg, 0.524 mmol), **17** (1.102 g, 0.578 mmol), CBr_4 (192 mg, 0.579 mmol), and DBU (172 μL, 1.152 mmol) in toluene (70 mL). After five days, the solvent was evaporated under reduced pressure, and the crude mixture separated by flash chromatography (SiO_2, toluene increasing to toluene/ethyl acetate 95:5) followed by preparative HPLC (SiO_2, toluene/ethyl acetate 98:2) to give the [60]fullerene – porphyrin-dendrimer **22** (12.8 mg, 2.0%). ^{1}H NMR (400 MHz, RT, $CDCl_3$): δ = 1.78 – 1.94 (m, 60H; dendrimer CH_2), 3.22 – 3.64 (m, 60H; dendrimer CH_2), 3.80 – 3.94 (m, 60H; dendrimer CH_2), 4.09 – 4.36 (m, 65H; dendrimer CH_2, porphyrin, CH_2, CH_3), 4.78 (br, 2H; CH_2 porphyrin), 4.91 – 4.82 (m, 80H; dendrimer CH_2), 6.22 – 6.53 (m, 90H; dendrimer ArH), 7.16 – 7.32 (m, 202H; dendrimer Ph, porphyrin Ph), 7.64 – 7.68 (m, 9H; porphyrin Ph), 8.05 (m, 2H; porphyrin Ph), 8.15 (m, 6H; porphyrin Ph), 8.87 – 8.91 (m, 8H; porphyrin β-pyrrole); ^{13}C NMR (100.5 MHz, RT, $CDCl_3$): δ = 28.85, 29.41, 29.63 (CH_2), 45.10, 45.33, 45.38, 45.68 (methano bridge), 50.88 (CH_3O), 63.72, 64.37, 64.74, 66.36, 66.53, 66.68, 66.91 (CH_2O), 69.17 (C_{60} sp^3 C), 69.88, 72.48, 72.64, 77.78 (CH_2O), 100.24, 101.17, 105.89, 106.30, 112.61 (arom. CH), 120.60, 120.79,

0947-6539/99/0508-2372 $ 17.50+.50/0 *Chem. Eur. J.* **1999**, *5*, No. 8

120.87 (porphyrin C), 126.42, 127.46, 127.87, 128.47 (PhCH), 131.81 (β-pyrrole CH), 134.48, 135.65 (PhCH), 136.76, 136.84 (PhC), 140.49, 140.56, 140.67, 140.79, 141.02 (arom. C), 141.23, 141.44, 141.47 (C_{60} sp^2 C), 143.07, 143.10 (β-pyrrole C), 145.78, 145.95, 146.08, 146.12 (C_{60} sp^2 C), 150.05, 150.10, 150.36 (PhC), 157.94, 159.91, 159.99, 160.04, 160.13, 160.25 (arom. C), 163.72, 164.16 (C=O); UV/Vis (CH_2Cl_2): $\lambda_{max} = 283$, 318 (sh), 336 (sh), 402 (sh), 425, 514, 552, 594 nm; IR (KBr): $\tilde{\nu} = 3062$, 3031, 2926, 2864, 1744, 1596, 1453, 1375, 1263, 1159, 1104, 1060, 831, 737, 697, 528 cm^{-1}.

Acknowledgements

This work was supported by the Stiftung Volkswagenwerk

[1] D. K. Smith, F. Diederich, *Chem. Eur. J.* **1998**, *4*, 1353.

[2] R.-H. Jin, T. Aida, S. Inoue, *J. Chem. Soc. Chem. Commun.* **1993**, 1261.

[3] a) P. J. Dandliker, F. Diederich, M. Gross, C. B. Knobler, A. Louati, E. M. Sanford, *Angew. Chem.* **1994**, *106*, 1821; *Angew. Chem. Int. Ed. Engl.* **1994**, *33*, 1739; b) P. J. Dandliker, F. Diederich, J.-P. Gisselbrecht, A. Louati, M. Gross, *Angew. Chem.* **1995**, *107*, 2906; *Angew. Chem. Int. Ed. Engl.* **1995**, *34*, 2906; c) P. J. Dandliker, F. Diederich, A. Zingg, J.-P. Gisselbrecht, M. Gross, A. Louati, E. Sanford, *Helv. Chim. Acta* **1997**, *80*, 1773.

[4] R. Sadamoto, N. Tomioka, T. Aida, *J. Am. Chem. Soc.* **1996**, *118*, 3978.

[5] P. Bhyrappa, J. K. Young, J. S. Moore, K. S. Suslick, *J. Am. Chem. Soc.* **1996**, *118*, 5708.

[6] B. Meunier, *Chem. Rev.* **1992**, *92*, 1411.

[7] a) B. R. Cook, T. J. Reinert, K. S. Suslick, *J. Am. Chem. Soc.* **1986**, *108*, 7281; b) K. S. Suslick, B. R. Cook, *J. Chem. Soc. Chem. Commun.* **1987**, 200.

[8] X. Camps, H. Schönberger, A. Hirsch, *Chem. Eur. J.* **1997**, *3*, 561.

[9] C. J. Hawker, J. M. J. Fréchet, *J. Am. Chem. Soc.* **1990**, *112*, 7638.

[10] a) P. A. Liddell, J. P. Sumida, A. N. Macpherson, L. Noss, G. R. Seely, K. N. Clark, A. L. Moore, T. A. Moore, D. Gust, *Photochem. Photobiol.* **1994**, *60*, 537; b) T. G. Linssen, K. Dürr, M. Hanack, A. Hirsch, *J. Chem. Soc. Chem. Commun.* **1995**, 103; c) H. Imahori, K. Hagiwara, T. Akiyama, S. Taniguchi, T. Okada, Y. Sakata, *Chem. Lett.* **1995**, 265; d) T. Drovetskaya, C. A. Reed, P. Boyd, *Tetrahedron Lett.* **1995**, *36*, 7971; e) H. Imahori, Y. Sakata, *Chem. Lett.* **1996**, 199; f) M. G. Ranasinghe, A. M. Oliver, D. F. Rothenfluh, A. Salek, M. N. Paddon-Row, *Tetrahedron Lett.* **1996**, *37*, 4797; g) H. Imahori, K. Hagiwara, M. Aoki, T. Akiyama, S. Taniguchi, T. Okada, M. Shirakawa, Y. Sakata, *J. Am. Chem. Soc.* **1996**, *118*, 11771; h) T. Akiyama, H. Imahori, A. Ajawakom, Y. Sakata, *Chem. Lett.* **1996**, 907; i) D. Kuciauskas, S. Lin, G. R. Seely, A. L. Moore, T. A. Moore, D. Gust, T. Drovetskaya, C. A. Reed, P. D. W. Boyd, *J. Phys. Chem.* **1996**, *100*, 15926; j) P. A. Liddell, D. Kuciauskas, J. P. Sumida, B. Nash, D. Nguyen, A. L. Moore, T. A. Moore, D. Gust, *J. Am. Chem. Soc.* **1997**, *119*, 1400; k) K. Dürr, S. Fiedler, T. Linßen, A. Hirsch, M. Hanack, *Chem. Ber. Recueil* **1997**, *130*, 1375; l) P. S. Baran, R. R. Monaco, A. U. Khan, D. J. Schuster, S. R. Wilson, *J. Am. Chem. Soc.* **1997**, *119*, 8363; m) H. Imahori, K. Yamada, M. Hasegawa, S. Taniguchi, T. Okada, Y. Sakata, *Angew. Chem.* **1997**, *109*, 2740; *Angew. Chem. Int. Ed. Engl.* **1997**, *36*, 2626; n) E. Dietel, A. Hirsch, J. Zhou, A. Rieker, *J. Chem. Soc. Perkin Trans. 2* **1998**, 1357; o) J.-F. Nierengarten, C. Schall, J.-F. Nicoud, *Angew. Chem.* **1998**, *110*, 2037; *Angew. Chem. Int. Ed.* **1998**, *37*, 1934; p) S. Higashida, H. Imahori, T. Kaneda, Y. Sakata, *Chem. Lett.* **1998**, 605; q) J.-F. Nierengarten, L. Oswald, J.-F. Nicoud, *Chem. Commun.* **1998**, 1545; r) E. Dietel, A. Hirsch, E. Eichhorn, A. Rieker, S. Hackbarth, B. Röder, *Chem. Commun.* **1998**, 1981.

[11] I. Lamparth, C. Mössmer, A. Hirsch, *Angew. Chem.* **1995**, *107*, 1755; *Angew. Chem. Int. Ed. Engl.* **1995**, *34*, 1607.

[12] A. Hirsch, *The Chemistry of the Fullerenes,* Thieme, Stuttgart, **1994**.

[13] K. L. Wooley, C. J. Hawker, J. M. J. Fréchet, *J. Am. Chem. Soc.* **1991**, *113*, 4252.

[14] D. Seebach, J.-M. Lapierre, G. Greiveldinger, K. Skobridis, *Helv. Chim. Acta* **1994**, *77*, 1673.

[15] D. Seebach, J.-M. Lapierre, K. Skobridis, G. Greiveldinger, *Angew. Chem.* **1994**, *106*, 457; *Angew. Chem. Int. Ed. Engl.* **1994**, *33*, 440.

[16] P. Murrer, D. Seebach, *Angew. Chem.* **1995**, *107*, 2297; *Angew. Chem. Int. Ed. Engl.* **1995**, *34*, 2116.

[17] H. M. Müller, D. Seebach, *Angew. Chem.* **1993**, *105*, 483; *Angew. Chem. Int. Ed. Engl.* **1993**, *32*, 477.

[18] A. Hermann, M. Rüttimann, C. Thilgen, F. Diederich, *Helv. Chim. Acta* **1995**, *78*, 1673.

[19] C. Bingel, *Chem. Ber.* **1993**, *126*, 1957.

[20] X. Camps, A. Hirsch, *J. Chem. Soc. Perkin Trans. 1* **1997**, 1595. For earlier modifications of the Bingel reactions see: C. Bingel, presentation at the meeting New Perspectives in Fullerene Chemistry and Physics, Rome, Italy, **1994** and J. F. Nierengarten, V. Gramlich, F. Cardullo, F. Diederich, *Angew. Chem.* **1996**, *108*, 2242; *Angew. Chem. Int. Ed. Engl.* **1996**, *35*, 2101.

[21] HYPERCHEM 4.5, Hypercube, **1995**, 419 Phillip Steet, Waterloo, Ontario N2l 3X2 (Canada).

[22] Molecular modeling was performed with the MM^+ method implemented in the HYPERCHEM software package. Geometry optimization with the Newton-Raphson algorithm was carried out connecting optimized addends to [60]fullerene in order to achieve optimized structures with high gradients.

[23] A 3 mm glassy carbon electrode was used as a working electrode, while silver/silver chloride (Ag/AgCl) was chosen as a reference electrode. Ferrocene was added as an internal potential reference, and all the values are reported vs. the Fc/Fc^+ couple. The compound concentration used was typically 0.4 mM. 100 mM $TBAPF_6$ (tetrabutylammonium hexafluorophosphate) was added as a supporting electrolyte after being recrystalized twice from ethanol/water (95/5%) and dried in vacuum. Dichloromethane was used as a solvent under an argon atmosphere. A typical scan rate was 100 $mV s^{-1}$, and the potentiostat used was a BAS 100 W electrochemical analyzer (Bioanalytical System) to make all electrochemical measurements.

[24] J.-P. Bourgeois, F. Diederich, L. Echegoyen, J.-F. Nierengarten, *Helv. Chim. Acta* **1998**, *81*, 1835.

[25] C. Boudon, J.-P. Gisselbrecht, M. Gross, A. Herrmann, M. Rüttimann, J. Crassous, F. Cardullo, L. Echegoyen, F. Diederich, *J. Am. Chem. Soc.* **1998**, *120*, 7860.

[26] a) C. Boudon, J.-P. Gisselbrecht, M. Gross, L. Isaacs, H. L. Anderson, R. Faust, F. Diederich, *Helv. Chim. Acta* **1995**, *78*, 1334; b) F. Cardullo, P. Seiler, L. Isaacs, J.-F. Nierengarten, R. F. Haldimann, F. Diederich, T. Mordasini-Denti, W. Thiel, C. Boudon, J.-P. Gisselbrecht, M. Gross, *Helv. Chim. Acta* **1997**, *80*, 343.

[27] In order to confirm whether energy or electron transfer occurs temperature dependent time-resolved picosecond fluorescence as well as picosecond transient absorption measurements were carried out. From these investigations, the electron transfer rate and the lifetime of the charge-separated state were calculated. These results will be published separately.

[28] a) B. Röder, Tetrapyrroles: A Chemical Class of Potent Photosensitizers for the Photodynamic Treatment of Tumours in *Laser Tumour Therapy* (Ed.: M. Trelles), Il. Col.Of. de Medicos de Madrid, **1990**, pp. (I-3)–(I-21); b) B. Röder, Individual data: Pheophorbides in *Quantitative data of 2nd and 3rd generation photosensitizers for Photodynamic Therapy - a laboratory manual*, (Ed.: J. G. Moser), Gordon and Breach Science, **1998**, pp. 35–42.

[29] H. Imahori, Y. Sakata, *Adv. Mater.* **1997**, *9*, 537.

[30] J. W. Arbogast, C. S. Foote, *J. Am. Chem. Soc.* **1991**, *113*, 8886.

[31] H. N. Ghosh, D. K. Palit, A. V. Sapre, J. P. Mittal, *Chem. Phys. Lett.* **1997**, *365*, 3–5.

[32] O. Korth, T. Hanke, B. Röder, *Thin Solid Films* **1998**, *320*, 305.

[33] W. Spiller, H. Kliesch, D. Wöhrle, S. Hackbarth, B. Röder *J. Porphyrins Phthalocyanines* **1998**, *2*, 145.

[34] S. Oelckers, M. Sczepan, T. Hanke, B. Röder *J. Photochem. Photobiol. B:Biology* **1997**, *39*, 219.

Received: December 7, 1998 [F1484]